Linear stability analysis of doubly diffusive vertical slot convection

Y. Young and R. Rosner
Department of Astronomy and Astrophysics, The University of Chicago, 5640 South Ellis Avenue, Chicago, Illinois 60637
(Received 20 January 1997; revised manuscript received 22 August 1997)

We examine the linear stability problem for slot convection in which several passive diffusing species are allowed for. Such systems show multiply diffusive behavior, in which convective instability leads to the formation of horizontal layers. Our analysis resolves discrepancies found in the literature of the physical interpretation of the initial instability. Our results are directly compared to existing experimental results, showing good agreement with the observed initial layer formation, including measured quantities such as layer thickness. Our results also show the importance of closely monitoring (and controlling) the horizontal temperature gradient, since the results are highly sensitive to this physical ingredient. [S1063-651X(98)05901-7]

PACS number(s): 47.20.Bp

I. INTRODUCTION

In this report we present results of linear stability analyses of the doubly diffusive slot convection problem [1–4]; our goal is to explain the layering seen in [5], where the horizontal temperature contrast is small and thermal conductivity is much larger than the solute diffusivities. In the weakly driven layering regime, a lateral thermal gradient is balanced by horizontal solute gradients, and a static state can be established in the interior of the tube. (A very small amplitude, narrow vertical boundary current is necessary to maintain the interior horizontal solute gradients [2,4].) As we shall show, extremely small temperature gradients suffice to place such systems into the layering regime; thus experiments that do not control temperature differences to the required level of precision may lead to misinterpretation of observed layering [6].

Results from our analysis are consistent with earlier work of [1] and [7]. When directly compared to the findings of [5], our results explain why large multiple layers first appear simultaneously in the middle of the tube, and we explain quantitatively how smaller layers form later, starting from the bottom. Furthermore, we show that the observation reported in [6] may be explained by triply diffusive slot convection in the weakly driven regime in the presence of a horizontal temperature difference as small as 0.1 mK, contrary to the interpretation presented in that work.

II. THE EQUATIONS

A. One stably stratified solute

We consider an infinitely tall two-dimensional (2D) system filled with incompressible fluid (the horizontal and vertical velocities u and w, respectively, are related to a stream function ϕ: $u=\partial_z\phi$ and $w=-\partial_x\phi$) as shown in Fig. 1, which we assume to be described by the following nondimensional equations within the Boussinesq approximation [11] [velocities are scaled by $\nu/(d/2)$, lengths by $d/2$, temperature by $\Delta T/2$, solute concentration by the vertical concentration difference $\gamma_c/2\equiv(d/2)|\partial_z C_0|$, where $\partial_z C_0$ is the initial vertical solute gradient, and time by $\nu/(d/2)^2$]

$$(\partial_t\nabla^2-\nabla^4)\phi+\frac{\mathrm{Gr}}{16}\partial_x T-\frac{\mathrm{Gr}_c}{16}\partial_x C-J(\phi,\nabla^2\phi)=0, \tag{2.1}$$

$$\left(\partial_t-\frac{1}{\mathrm{Pr}}\nabla^2\right)T-J(\phi,T)=0, \tag{2.2}$$

$$\left(\partial_t-\frac{1}{\mathrm{Pr}_c}\nabla^2\right)C-J(\phi,C)=0. \tag{2.3}$$

$J(f,g)\equiv\partial_x f\partial_z g-\partial_z f\partial_x g$ is the Jacobian; the thermal Grashof number $\mathrm{Gr}\equiv g\alpha\Delta T d^3/\nu^2$; the solute Grashof number $\mathrm{Gr}_c\equiv g\beta_c\gamma_c d^3/\nu^2$; the thermal Prandtl number $\mathrm{Pr}=\nu/\kappa_t$, and the solute Prandtl number $\mathrm{Pr}_c=\nu/\kappa_c$ (thermal Rayleigh number $\mathrm{Ra}_t=\mathrm{Gr}\times\mathrm{Pr}$ and solute Rayleigh number $\mathrm{Ra}_c=\mathrm{Gr}_c\times\mathrm{Pr}_c$). Other dimensional constants are the thermal expansion coefficient α, the solute volumetric expansion coefficient β_c, the thermal diffusivity κ_t, the solute diffusivity κ_c, the kinematic viscosity ν, and the gravitational acceleration g. We adopt boundary conditions for impenetrable, no-slip vertical walls fixed at constant temperatures (Fig. 1). We approximate the unperturbed state (subscript ''0'') by a static

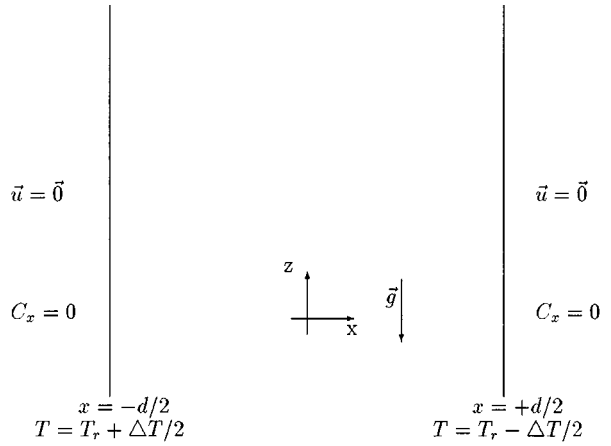

FIG. 1. Conceptual sketch of the vertical slot filled with stably stratified solute: $\beta_c\cdot\partial_z C_0=\text{constant}<0$.

state: $\phi_0=0$, $T_0(x,z)=T_r-\Delta T/dx$, $\partial_x C_0=-\alpha\Delta T/\beta_c d$, and $\beta_c\partial_z C_0\leqslant 0$, where T_r is a reference temperature (e.g., room temperature). As shown in [4] for solute Rayleigh number $\mathrm{Ra}_c>10^6$, linear analysis with this quasistatic approximation gives essentially the same results as those without this approximation. (In [5] and [6], $\mathrm{Ra}_c>10^8$ because $\kappa_c\leqslant 10^{-8}$.) The linearized equations are then

$$\partial_t\nabla^2\phi=\nabla^4\phi-\frac{\mathrm{Gr}}{16}\,\partial_x T+\frac{\mathrm{Gr}_c}{16}\,\partial_x C, \tag{2.4}$$

$$\partial_t T=\partial_z\phi+\frac{1}{\mathrm{Pr}}\,\nabla^2 T, \tag{2.5}$$

$$\partial_t C=\frac{\mathrm{Gr}}{\mathrm{Gr}_c}\,\partial_z\phi+\frac{\partial_z C_0}{|\partial_z C_0|}\,\partial_x\phi+\frac{1}{\mathrm{Pr}_c}\,\nabla^2 C. \tag{2.6}$$

In [5] and [6] the Schmidt number $H_c\equiv\kappa_t/\kappa_c=\mathrm{Pr}_c/\mathrm{Pr}$ is much larger than 1 (10^5–10^6); thus one may consider the temperature to remain unperturbed during the entire experiment, and Eqs. (2.4)–(2.6) can be simplified to read

$$\partial_t\nabla^2\phi=\nabla^4\phi+\frac{\mathrm{Gr}_c}{16}\,\partial_x C, \tag{2.7}$$

$$\partial_t C=\frac{\mathrm{Gr}}{\mathrm{Gr}_c}\,\partial_z\phi+\frac{\partial_z C_0}{|\partial_z C_0|}\,\partial_x\phi+\frac{1}{\mathrm{Pr}_c}\,\nabla^2 C. \tag{2.8}$$

In the case where solute C_0 is neutrally stratified, we obtain [C scaled by $|\alpha\Delta T/(2\beta_c)|$]

$$\partial_t\nabla^2\phi=\nabla^4\phi\pm\frac{\mathrm{Gr}}{16}\,\partial_x C, \tag{2.9}$$

$$\partial_t C=\pm\,\partial_z\phi+\frac{1}{\mathrm{Pr}_c}\,\nabla^2 C, \tag{2.10}$$

where $+$ is for $\beta_c>0$ and $-$ is for $\beta_c<0$.

B. Two stably stratified solutes

We now add one more stabilizing solute into our system as done in the experiments of [6]. The two solutes are denoted by C and S, scaled by the vertical concentration difference $\gamma_c\equiv(d/2)|\partial_z C_0|$ and $\gamma_s\equiv(d/2)|\partial_z S_0|$, respectively. With the same scalings as in previous cases, we have (in the limiting case where the two Schmidt numbers $H_c=\kappa_t/\kappa_c=\mathrm{Pr}/\mathrm{Pr}_c$ and $H_s=\kappa_t/\kappa_s=\mathrm{Pr}/\mathrm{Pr}_s$ are both much larger than 1)

$$\partial_t\nabla^2\phi=\nabla^4\phi+\frac{\mathrm{Gr}_s}{16}\,\partial_x S+\frac{\mathrm{Gr}_c}{16}\,\partial_x C, \tag{2.11}$$

$$\partial_t S=\frac{\mathrm{Gr}}{\mathrm{Gr}_c}\,\frac{\mathrm{Pr}_s}{\mathrm{Pr}_c}\,\partial_z\phi-\partial_x\phi+\frac{1}{\mathrm{Pr}_s}\,\nabla^2 S, \tag{2.12}$$

$$\partial_t C=\frac{\mathrm{Gr}}{\mathrm{Gr}_c}\,\partial_z\phi-\partial_x\phi+\frac{1}{\mathrm{Pr}_c}\,\nabla^2 C. \tag{2.13}$$

Coefficients of the first terms on the right-hand side of Eqs. (2.12) and (2.13) are the initial lateral gradients of S and C, respectively; these two lateral gradients combine to balance the horizontal temperature gradient.

III. NUMERICS

We use the spectral method [12,13] to solve the equations presented in the previous section. We assume an $e^{\lambda t}$ dependence, and expand spatial terms in Fourier-Chebychev series (Chebychev in x and Fourier in z). On introducing an auxiliary function $\omega=\nabla^2\phi$ to reduce the order of differentiation and thus retain numerical accuracy, we arrive at the generalized eigenvalue equation

$$\mathbf{A}\cdot\mathbf{x}=\lambda\mathbf{B}\cdot\mathbf{x}, \tag{3.1}$$

where $\mathbf{A}$ and $\mathbf{B}$ are square matrixes obtained from the equations in the previous section, and $\mathbf{x}$ is a vector composed of ϕ, ω, T, C, and S. The matrix $\mathbf{A}$ is a function of control parameters $(\mathrm{Gr},\mathrm{Gr}/\mathrm{Gr}_c,\mathrm{Pr},\mathrm{Pr}_c)$ for Eqs. (2.4)–(2.6), $(\mathrm{Gr},\mathrm{Gr}/\mathrm{Gr}_c,\mathrm{Pr}_c)$ for Eqs. (2.7) and (2.8), and $(\mathrm{Gr}/\mathrm{Gr}_c,\mathrm{Gr}_c,\mathrm{Gr}_s,\mathrm{Pr}_c,\mathrm{Pr}_s)$ for Eqs. (2.11)–(2.13). Boundary conditions $\phi=\partial_x\phi=T=\partial_x C=\partial_x S=0|_{x=\pm 1}$ are incorporated into Eq. (3.1) using the tau approximation [13]. We solve this equation (with the solver from the LAPACK package) in the full parameter space to find neutral stability curves. Our numerical solutions exhibit good resolution when we increase the number of modes (i.e., the spectrum shows power-law decay and remains flat at the higher end) and the convergence is satisfactory when we use as few modes as 32.

IV. RESULTS

We examine two cases: first, the ''creaming emulsion'' experiments [5], where $\beta_c=-0.27<0$, $\mathrm{Pr}=7.5$, and $\mathrm{Pr}_c=10^6$–$10^7\gg 1$; second, the ''sedimenting polystyrene'' experiments of [6], for which $\beta_c=0.054$, $\mathrm{Pr}=7.5$, and $\mathrm{Pr}_c\sim 2.563\times 10^6$. The lower limit on $\mathrm{Pr}_c(=10^6)$ for the first case is obtained when κ_c is the Brownian diffusivity [14]; the upper limit $(=10^7)$ comes from the results of [8] $\kappa_c\sim k' a V_0$ [with k' an empirical coefficient of order $O(1)$] and from [5] that the creaming velocity $V_0=0.26\ \mu\mathrm{m\ s}^{-1}$, and the radius of the colloids $a=0.6\ \mu$m. In the second case, we presume polystyrene spheres of diameter $\sim 1.091\ \mu$m [6], and adopt the Brownian diffusivity for κ_c.

A. ''Creaming emulsion'': One stably stratified solute

First for $\partial_z C_0>0$, we present calculations carried out for values of the control parameters lying in the range explored by the laboratory experiments: $\beta_c=-0.27$, $\mathrm{Pr}_c=10^6$–10^7, $\nu=0.01\ \mathrm{cm^2\ s^{-1}}$ for water, and the ratio $|\mathrm{Gr}/\mathrm{Gr}_c|$ in the range 0.1–1.0. Regardless of whether thermal diffusion is included in the equations, we find that the critical Grashof numbers and critical vertical wave numbers are almost the same for $\mathrm{Pr}_c=10^6$–10^7; thus we show (Fig. 2) the neutral stability curve for calculations of Eqs. (2.4)–(2.6) using 32 modes and the parameter values $\mathrm{Gr}/\mathrm{Gr}_c=-0.18$, $\mathrm{Pr}_c=10^7$, $\mathrm{Pr}=\nu/\kappa_t=7.5$. In Fig. 3(a) we show the marginal stability

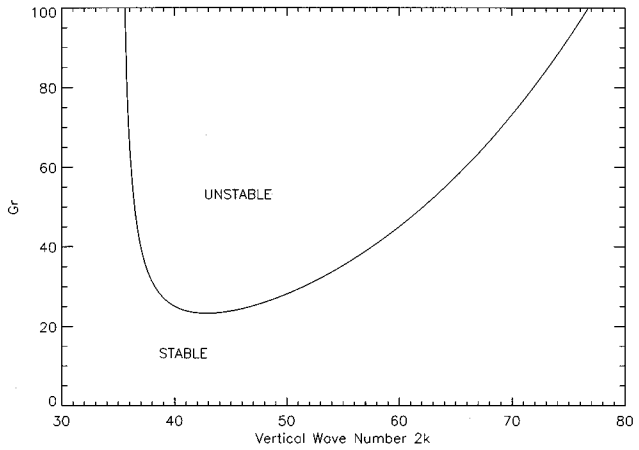

FIG. 2. Plot of the neutral stability curve for the system of Eqs. (2.4)–(2.6), for $\mathrm{Gr}/\mathrm{Gr}_c=-0.18$, $\mathrm{Pr}_c=10^7$, $\mathrm{Pr}=\nu/\kappa_t=7.5$; 32 modes were used ($2\times k$ because we scale the length by $d/2$). The corresponding critical wavelength is $\lambda_{\mathrm{crit}}=1.47$ mm and critical lateral temperature difference is $\Delta T_{\mathrm{crit}}=10.7$ mK for a tube width $d=1$ cm in [5]. The lateral temperature difference in [5] is 10 ± 2 mK; the observed small strata near the bottom of the tube have thickness $1\sim2$ mm.

curve in the $\mathrm{Ra}_t-\mathrm{Ra}_c$ plane for $\mathrm{Pr}=7.5$, $\mathrm{Pr}_c=10^7$; Fig. 3(b) shows the critical wave number as a function of Ra_c ($\mathrm{Ra}_t=\mathrm{Gr}\times\mathrm{Pr}$, $\mathrm{Ra}_c=\mathrm{Gr}_c\times\mathrm{Pr}_c$). In the case of $\partial_z C_0=0$, results of our calculation show that for all values of $\mathrm{Pr}_c=10^6-10^7$, the critical wavelength $\lambda_{\mathrm{crit}}\sim2.5$ cm for $d=1$ cm [5] and the critical Grashof numbers are very small ($\mathrm{Gr}_c\sim10^{-2}$ for $\mathrm{Pr}_c=10^6$).

The results above can explain layering observed in [5]. Some large layers of thickness 2–3 cm appear first in the middle of the tube; this is easily understood as a consequence of the fact that the suspension is nearly neutrally stratified there, and hence layers form first due to the small critical lateral temperature contrast. Smaller (1–2 mm) strata appear near the bottom of the tube because, while the temperature difference is kept constant throughout the experiment (fixed Ra_t), the emulsion floats upwards at a creaming velocity of $0.26\ \mu\mathrm{m\ s}^{-1}$ from the bottom; and since this is much faster than the diffusion velocity ($\equiv\kappa_c/l_c=10^{-4}-10^{-3}\ \mu\mathrm{m\ s}^{-1}$, where l_c, the characteristic length, is 1–2 mm), one would expect a vertical discontinuity in the density of the emulsion during the creaming process near the bottom. Thus, the vertical gradient of the concentration field behaves like a delta function at this discontinuity. At the peak of the vertical gradient (the discontinuity), the system is stable because the solute Rayleigh number $-\mathrm{Ra}_c$ is very large there. However, diffusion of the solute will smooth out the vertical gradient (thus decreasing the solute Rayleigh number $-\mathrm{Ra}_c$ at the discontinuity) on a time scale of $t\sim l_c^2/(3\pi^2\kappa_c)$ [14], and as soon as the gradient becomes constant over l_c and has a value such that $-\mathrm{Ra}_c$ crosses the marginal curve, instability sets in and the layering begins. Adopting $\kappa_c=(1-2)\times10^{-9}\ \mathrm{cm^2\ s^{-1}}$ and $l_c\sim1$ mm, we obtain a time scale of 2.0–4.0 d for small strata to appear near the bottom of the column, in good agreement with the experiments [5].

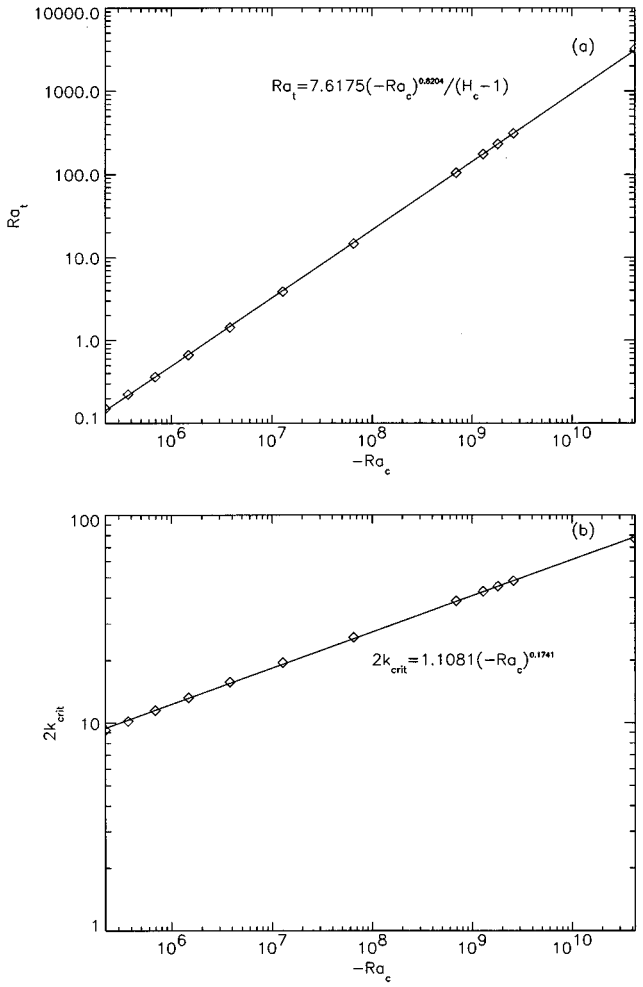

FIG. 3. Panel (a): Marginal stability curve for $\mathrm{Pr}=7.5$, $\mathrm{Pr}_c=10^7$, $\mathrm{H}_c=\mathrm{Pr}_c/\mathrm{Pr}=1.3\times10^6$; 32 modes were used in calculating Eq. (3.1). The best-fit line is given by $\mathrm{Ra}_t=7.6175\times(-\mathrm{Ra}_c)^{0.8204}/(H_c-1)$, consistent with results of [7], $\mathrm{Ra}_t=5.8977\times(-\mathrm{Ra}_c)^{5/6}/(H_c-1)$. For a fixed Ra_t (fixed lateral temperature difference), the system is stable for $-\mathrm{Ra}_c>-\mathrm{Ra}_{c,\mathrm{crit}}$ and unstable for $-\mathrm{Ra}_c<-\mathrm{Ra}_{c,\mathrm{crit}}$, where $-\mathrm{Ra}_{c,\mathrm{crit}}=(\mathrm{Ra}_t\times(H_c-1)/7.6175)^{1/0.8204}$. Panel (b): Critical wave number $2\times k_{\mathrm{crit}}$ as a function of $-\mathrm{Ra}_c$ ($2\times k_{\mathrm{crit}}$ because we scale lengths by the half slot width). The best-fit line is given by $2\times k_{\mathrm{crit}}=1.1081\times(-\mathrm{Ra}_c)^{0.1741}$, consistent with results of [1] and [7], $k_{\mathrm{crit}}=1.3048\times(-\mathrm{Ra}_c)^{1/6}$.

Finally, we remark that it is not straightforward to apply the results of linear stability analyses in [1–4] to the layer formation near horizontal boundaries, where both the vertical saline flux and the vertical flow fall to zero. The assumed initial vertical boundary current (required to sustain the interior lateral solute gradient) increases in amplitude as the solute Rayleigh number $|\mathrm{Ra}_c|$ decreases [2–4]. Thus the unperturbed flow cannot be purely vertical near the horizontal boundaries where $|\mathrm{Ra}_c|$ begins to decrease [10], and the appearance of layers in these regions [1,9] may not be completely explained by the linear stability analysis where the initial flow is assumed vertical [2–4]. In the case of a creaming emulsion, this assumption holds well at the concentration discontinuity where small strata begin to appear [5], and the comoving creaming velocity of the emulsion further guaran-

tees that the formation of small strata can only occur near the bottom.

B. ''Sedimenting polystyrene'': Two stably stratified solutes

As in Table I of [6], we adopt $\beta_c = 0.054$ and $\mathrm{Pr}_c = 2.563 \times 10^6$. Calculations show that for linearly stratified 1.1 μm polystyrene and salt (both zero concentration at the top of the tube and 0.1 wt % at the bottom), the lower bound on the lateral temperature contrast for layering is 0.1 mK and the critical wavelength is 0.5 cm for a tube width of 0.6 cm, in good agreement with Siano's result (Table I in [6]). The salt will remain unperturbed if it is initially uniform; thus one expects the layer width observed with a uniform salt background to be the same as that without salt (Table I in [6]). In this case our calculations show that the critical lateral temperature difference is as small as 0.01 mK and the critical wavelength is 1.3 cm for $d = 0.6$ cm, in good agreement with Table I of [6]. Reference [6] also describes the average layer width as a function of concentration for 1.091 μm diameter polystyrene spheres, with an initially linear vertical concentration gradient of polymer and a homogeneous salt concentration; our results for this particular set of parameters are also in good agreement with this measurement, suggesting that the multidiffusive slot convection model is indeed a good description of these experiments.

V. CONCLUSIONS

We have examined the linear stability problem for slot convection in which additional stably stratified solutes are sustained by a narrow vertical boundary current to balance the imposed lateral temperature gradient. Focusing on the weakly driven regime, we have explained the layering seen in [5], with estimates for both layer thickness in various locations and the time scale for the appearance of small strata, in good agreement with the observations. The demonstration of the remarkably small horizontal thermal gradients, which suffice to result in layering, confirms the point addressed in [5]: the (very small) temperature gradients were most likely not properly measured (or controlled) in the early experiments, leading to misinterpretations of the governing physics. Thus, it appears likely that [6] is incorrect in concluding that convection is not responsible for the observed layering.

ACKNOWLEDGMENTS

We would like to thank J. Biello, F. Cattaneo, T. Dupont, D. Grier, and A. E. Hosoi for helpful conversations; this work was supported in part by NASA grants to the University of Chicago.

[1] S. A. Thorpe, P. K. Hutt, and R. Soulsby, J. Fluid Mech. **38**, 375 (1969).
[2] J. E. Hart, J. Fluid Mech. **49**, 279 (1971).
[3] S. Thangam, A. Zebib, and C. F. Chen, J. Fluid Mech. **112**, 151 (1981).
[4] R. C. Paliwal and C. F. Chen, J. Fluid Mech. **98**, 769 (1980).
[5] D. M. Mueth, J. C. Crocker, S. E. Esipov, and D. G. Grier, Phys. Rev. Lett. **77**, 578 (1996).
[6] D. B. Siano, J. Colloid Interface Sci. **68**, 111 (1979).
[7] J. E. Hart, J. Fluid Mech. **59**, 47 (1973).
[8] S. E. Esipov, Phys. Rev. E **52**, 3711 (1995).
[9] C. F. Chen, D. G. Briggs, and R. A. Wirtz, Int. J. Heat Mass Transf. **14**, 57 (1971).
[10] Jin Wook Lee and Jae Min Hyun, Int. J. Heat Mass Transf. **34**, 2409 (1991).
[11] S. Chandrasekhar, *Hydrodynamic and Hydromagnetic Stability* (Dover Publication, New York, 1981).
[12] A. H. McAllister, Ph.D. thesis, The University of Texas at Austin, 1991.
[13] C. Canuto, M. Y. Hussaini, A. Quarteroni, and T. A. Zang, *Spectral Methods in Fluid Dynamics* (Springer Verlag, New York, 1988).
[14] L. D. Landau and E. M. Lifshitz, *Fluid Mechanics* (Pergamon Press, Oxford, 1959).